2013 European Control Conference (ECC)
July 17-19, 2013, Zürich, Switzerland.

Reducing Domain Structural Complexity in PDE Backstepping Boundary Observer Design using Conformal Mapping

Reza Banaei Khosroushahi, *Student Member, IEEE,* and Horacio J. Marquez, *Senior Member, IEEE*

***Abstract*— In this paper we study backstepping boundary observer design for a class of distributed parameter systems defined in a cylindrical domain with prescribed boundary conditions. We show that applying standard PDE backstepping boundary observer design results in a hyperbolic PDE with four independent variables which is difficult to solve both numerically and analytically. By introducing a modified domain structure using conformal mapping, we obtain a simplified design process which is reduced to solving a two-dimensional PDE for the kernel function. Finally, we sketch the complete treatment to solve the partial differential equation describing the kernel equation and then perform a simulation study to verify the L^2 performance of the designed observer. This technique has a direct application in soft-sensor design for internal temperature measurement in systems subjected to dynamic heat distribution, particularly microfluidic Lab-on-a-Chip (LOC) devices.**

I. INTRODUCTION

Observer design for infinite-dimensional systems is a challenging problem. Research on control and state estimator design for distributed parameter systems can be traced back to the 1960s and 70s [1]. Kitamura *et al.* [2], and Gressang and Lamont [3] developed conditions to generalize observer theory to infinite dimensional systems. El Jai and Amouroux [4] showed that because of the distributed nature of the problem, sensor location can have a detrimental effect on the observer existence. Liu and Lapidus [5] incorporated a Lyapunov-based observer design for linear and non-linear distributed-parameter diffusion systems. Yaz *et al.* [6] introduced the receding-window observer that has a structure similar to a Kalman filter and proved its convergence in the presence of bounded noises and parameter perturbation. Miranda *et al.* [7] proposed a sliding-mode observer by adding the sliding-mode term to the PDE backstepping boundary observer. This method is further developed for feedback stabilization [8]. A recent survey on the observers for distributed parameter systems can be found in [9].

Very recently, Krstić *et al.* generalized the well-known *Backstepping* approach for controller design for the systems that are described by partial differential equations [10], [11]. An important feature of this approach is the constructive nature of the design, which uses classical Lyapunov stability theory, making the design process relatively straightforward. However, this generalization deals exclusively with one-dimensional systems. Extensions to higher order systems are nontrivial as the complexity of the approach can quickly make the problem intractable. Some general guidelines for special systems in two and three dimensions are mentioned in reference [12], but in general, backstepping control for high-order PDE systems remains unsolved.

Our interest in this paper is to propose an extension of the backstepping boundary design for a specific class of PDE systems. We tackle observer design by using a conformal transformation that converts the original two-dimensional problem into an equivalent problem in one dimension, for which a solution is readily available. Our approach in the original form can be extended to other classes of PDE systems.

II. PROBLEM FORMULATION

Consider the following system:

$$u_t(\rho,z,t) = u_{\rho\rho}(\rho,z,t) + \frac{1}{\rho}u_\rho(\rho,z,t) + \eta\, u_{zz}(\rho,z,t), \quad (1a)$$

where $u : U \longrightarrow \mathbb{R}^+$, $U = \{\rho,\phi,z : \rho,z \in (0,1), \phi \in [0,2\pi]\}$, and subject to the following initial condition and boundary conditions:

$$u(\rho,z,0) = u_0(\rho,z) \qquad \rho,z \in [0,1] \quad (1b)$$
$$u(1,z,t) = 0 \qquad t \geq 0,\ z \in [0,1] \quad (1c)$$
$$u_\rho(0,z,t) = 0 \qquad t \geq 0,\ z \in [0,1] \quad (1d)$$
$$u_z(\rho,1,t) = 0 \qquad t \geq 0,\ \rho \in [0,1] \quad (1e)$$
$$u_z(\rho,0,t) = f(\rho)\,\delta U. \qquad t \geq 0,\ \rho \in [0,1] \quad (1f)$$

We are interested in designing a distributed parameter observer to estimate the value of $u(\rho,z,t)$ by knowing its boundary values. We dropped spatial variable ϕ in our equations due to symmetry toward ϕ axis in the domain. $u_0(\rho,z)$ describes the initial values of u, δU is the normalized input power and $f(\rho)$ describes the structural distribution of the input energy at the bottom boundary as follows:

$$f(\rho) = \begin{cases} 1 & \text{if } k_1 < \rho < (k_1+k_2) \\ 0 & \text{otherwise} \end{cases} \quad (2)$$

In contrast to simpler cases discussed in the literature, i.e. [13], where energy flow happens between two parallel boundaries, our system features energy flow between bottom and side boundaries which are geometrically perpendicular.

The normalized system (1) can be visualized as the thermal system depicted in Fig. 1 where the temperature inside the domain is represented by $\bar{u} : V \longrightarrow \mathbb{R}^+$ where $V = \{\bar{\rho},\bar{\phi},\bar{z} : \bar{\rho} \in (0,a), \bar{\phi} \in [0,2\pi], \bar{z} \in (0,b)\}$, which is governed by the heat conduction equation, $\kappa\nabla^2\,\bar{u} = \frac{\partial \bar{u}}{\partial t}$, where κ is thermal diffusivity. The transformation between the thermal system

The authors are with the Department of Electrical and Computer Engineering, University of Alberta, Edmonton, AB T6G 2V4, Canada (e-mail: banaeikh@ualberta.ca; hmarquez@ualberta.ca)

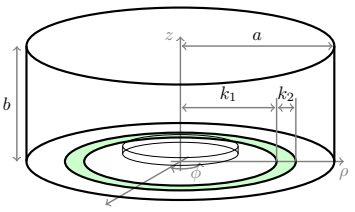

Fig. 1: Model Structure

and normalized system (1) can be carried out by scaling spatial variables $\bar{\rho}$ and $\bar{z}$, and temporal variable $\bar{t}$ to $\rho = \frac{\bar{\rho}}{q}$, $z = \frac{\bar{z}}{b}$ and $t = \frac{\kappa \bar{t}}{a^2}$ respectively. We also have $\eta = \frac{a^2}{b^2}$, $k_1 = \frac{k_1}{a}$ and $k_2 = \frac{k_2}{a}$.

For the sake of readability, from this point on we will drop the notation for the time in our equations.

III. PRELIMINARY RESULTS: PDE BACKSTEPPING BOUNDARY OBSERVER DESIGN

For the PDE model (1), the PDE backstepping boundary observer takes the following form [11]:

$$\hat{u}_t(\rho,z) = \hat{u}_{\rho\rho}(\rho,z) + \frac{1}{\rho}\hat{u}_\rho(\rho,z) + \eta\,\hat{u}_{zz}(\rho,z) + \ell(\rho,z)(u(\rho,0) - \hat{u}(\rho,0)), \qquad \rho,z \in (0,1) \quad (3a)$$

along with the following boundary conditions:

$$\hat{u}(1,z) = 0 \qquad z \in [0,1] \quad (3b)$$
$$\hat{u}_\rho(0,z) = 0 \qquad z \in [0,1] \quad (3c)$$
$$\hat{u}_z(\rho,1) = 0 \qquad \rho \in [0,1] \quad (3d)$$
$$\hat{u}_z(\rho,0) = f(\rho)\cdot\delta U + \ell_a.(u(\rho,0) - \hat{u}(\rho,0)), \qquad \rho \in [0,1] \quad (3e)$$

where $\ell(\rho,z)$ and ℓ_a are the observer parameters. Introducing the error $\tilde{u}(\rho,z) = u(\rho,z) - \hat{u}(\rho,z)$, calculating the PDE equation of the error dynamics results in:

$$\tilde{u}_t(\rho,z) = \tilde{u}_{\rho\rho}(\rho,z) + \frac{1}{\rho}\tilde{u}_\rho(\rho,z) + \eta\,\tilde{u}_{zz}(\rho,z) - \ell(\rho,z)\tilde{u}(\rho,0), \qquad \rho,z \in (0,1) \quad (4a)$$

with the same boundary conditions (4b)-(4d) and substituting (4e) with

$$\tilde{u}_z(\rho,0) = -\ell_a\tilde{u}(\rho,0), \qquad \rho \in [0,1] \quad (4b)$$

The observer design problem is to determine the observer parameters $\ell(\rho,z)$ and ℓ_a such that the estimation error asymptotically converges to zero at all points in the domain. We look for an integral transformation of the form

$$\tilde{u}(\rho,z) = \tilde{w}(\rho,z) - \int_\rho^1 \int_0^z P(\rho,\xi_1,z,\xi_2)\tilde{w}(\xi_1,\xi_2)\,\xi_1 d\xi_2 d\xi_1, \quad (5)$$

to transform the error dynamics into the following exponentially stable target system:

$$\tilde{w}_t(\rho,z) = \tilde{w}_{\rho\rho}(\rho,z) + \frac{1}{\rho}\tilde{w}_\rho(\rho,z) + \eta\,\tilde{w}_{zz}(\rho,z), \qquad \rho,z \in (0,1) \quad (6a)$$

subject to the following boundary conditions:

$$\tilde{w}(1,z) = 0 \qquad z \in [0,1] \quad (6b)$$
$$\tilde{w}_\rho(0,z) = 0 \qquad z \in [0,1] \quad (6c)$$
$$\tilde{w}_z(\rho,1) = 0 \qquad \rho \in [0,1] \quad (6d)$$
$$\tilde{w}_z(\rho,0) = 0. \qquad \rho \in [0,1] \quad (6e)$$

The following theorem states that the observer parameters $\ell(\rho,z)$ and ℓ_a can be defined by the integral kernel $P(\rho,\xi_1,z,\xi_2)$.

Theorem 1: Consider that the PDE observer error dynamics in 2-D cylindrical domain is defined by (4). Suppose that there exists an integral transformation (5) that transforms the error dynamics into (6). In addition, suppose that $P(\rho,\xi_1,z,\xi_2)$ as the kernel of integral transformation where $0 \le \rho \le \xi_1 \le 1$ and $0 \le \xi_2 \le z \le 1$ describe the domain of the kernel function. Then, the observer parameters $\ell(\rho,z)$ and ℓ_a can be explicitly defined by the kernel function, $P(\rho,\xi_1,z,\xi_2)$, and the kernel function itself can be calculated by solving the following PDE equation:

$$P_{\rho\rho} + \frac{1}{\rho}P_\rho + \eta P_{zz} = P_{\xi_1\xi_1} + \frac{1}{\xi_1}P_{\xi_1} + \eta P_{\xi_2\xi_2}, \quad (7a)$$

with the following boundary conditions:

$$\rho\frac{d}{d\rho}P(\rho,\rho,z,\xi_2) + P(\rho,\rho,z,\xi_2) = 0 \quad (7b)$$
$$\frac{d}{dz}P(\rho,\xi_1,z,z) = 0 \quad (7c)$$
$$P_\rho(0,\xi_1,z,\xi_2) = 0 \quad (7d)$$
$$P_z(\rho,\xi_1,1,\xi_2) = 0 \quad (7e)$$
$$P(\rho,1,z,\xi_2) = 0 \quad (7f)$$
$$P(\rho,\xi_1,1,1) = 0. \quad (7g)$$

Proof: Due to space limitations, the proof is not provided here. The detailed proof is available upon request from the authors. ■

Remarks: A simple inspection of the PDE (7) shows it has four independent variables. The solution to this 4-D PDE is, in general, very difficult to solve either analytically or numerically. In the next section, we use a conformal transformation to simplify the domain structure of the system (1) resulting in a 2-D PDE for kernel function.

IV. MAIN RESULTS

In this section, we modify the structure of the problem to relax one of the independent variables in the original system. The observer designed for the transformed system and the original state variable can be obtain by reverting back to the original. The block diagram shown in Fig. 2 illustrates the process.

We begin by investigating the spatial distribution of the function $u(\rho,z)$ in system (1) in our problem: Fig. 3a shows the energy flux lines and constant value lines in the domain. Energy flux lines and constant value lines are solutions to the orthogonal functions in an infinite series describing system (1). Therefore, energy flux lines and constant value lines always intersect at 90°angles. The central idea to our

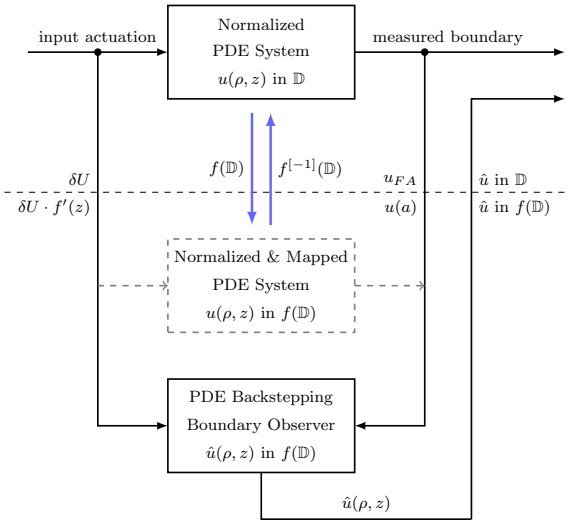

Fig. 2: Interconnection between the observer designed for the mapped PDE system and the original normalized PDE system

approach consists of finding a transformation that maps the present domain structure into a new one in which flux lines and constant value lines are straight lines intersecting at 90°angles. According to standard results in the theory of complex variables, such transformation is known as *conformal transformation* or *conformal mapping* [14]. A key element in the process of using conformal mapping for the class of the system introduced in section II is that the Laplace equation governing the function in the domain is invariant under conformal mapping.

Throughout this section we use the following notations: $\{\Omega_z; z_1, z_2, z_3, z_4\}$ denotes a generalized quadrilateral in the complex plane where Ω_z is a Jordan region and four distinguished points, z_1,z_2,z_3 and z_4, lying in order on the boundary. Essential background material can be found in [14].

A. CONFORMAL MAPPING

We are interested in a transformation to map the six vertex $[A, B, C, D, E, F]$ polygon shown in Fig. 3a into a new coordinate system. It follows from the *Riemann mapping theorem* that a mapping function exists which takes the initial domain shown in Fig. 3a to the simpler domain shown in Fig. 3c [15]. The six segments that define this polygon, namely $[AB]$, $[BC]$, $[CD]$, $[DE]$, $[EF]$, and $[FA]$, intersect at points B, C, D, and E, with 90° angles and at points F and A with 180° angles. To this end, we break down the problem into two steps:

1) Find the mapping, f_1, which transforms the initial geometry shown in Fig. 3a to the auxiliary geometry shown in Fig. 3b.
2) Find the mapping, f_2, which transforms the auxiliary geometry to the final geometry depicted in Fig. 3c.

The initial geometry is a generalized quadrilateral defined by $Q := \{\Omega_w; A, B, C, F\}$ and resembles the domain of system (1). The auxiliary geometry, defined by $R := \{\Omega_z; \tilde{a} + i\tilde{b}, -\tilde{a} + i\tilde{b}, -\tilde{a}, \tilde{a}\}$, is a rectangle symmetrically placed about the y-axis in z-plane depicted in Fig. 3b.

The first step itself can be broken down into three steps. We first find the mapping, f_{11}, which maps Q to the upper half plane denoted by H^+. Mapping f_{11} is given by the inverse Schwarz-Christoffel transformation [16].

The mapping f_{11} transforms vertices A,B,C and F into z_1, z_2, z_3 and z_4, which are laid out in order on the real axis. Next we use a Möbius transformation, f_{12}, to reorder z_1, z_2, z_3 and z_4 so that they are placed at $\frac{1}{k}$, $-\frac{1}{k}$, -1 and 1, respectively for some $k \in (0, 1)$. This transformation is essential to the next step. The next step is to find the mapping, f_{13}, to map the domain represented by H^+ and the critical points in $\frac{1}{k}$, $-\frac{1}{k}$, -1 and 1 onto the auxiliary domain R. This transformation is defined by the elliptic integral of the first kind [16]. The composition of f_{11}, f_{12} and f_{13} construct mapping f_1,

$$f_1(z) = f_{13} \circ f_{12} \circ f_{11}(z). \tag{8}$$

The mapping, $f_1(z)$, is called canonical mapping of the quadrilateral Q. The transformation from the canonical rectangle to the final geometry can be easily carried out by the following linear mapping performing rotation, translation and stretching:

$$f_2(z) = \frac{1}{\tilde{b}} z + 1 - \frac{\tilde{a}}{\tilde{b}} + i, \tag{9}$$

where $\tilde{a}$ and $\tilde{b}$ are calculated as $\tilde{a} = 1.7017$ and $\tilde{b} = 2.1079$.

Finally, the mapping $g(z)$ from the initial geometry to the final geometry is defined by the composition of the mapping, f_2, and the inverse mapping, f_1, as follows:

$$g(z) := f_2 \circ f_1(z). \tag{10}$$

Calculating the forward and inverse Schwarz-Christoffel mappings requires certain numerical considerations. These considerations are well implemented in the SC Toolbox for MATLAB written by T. A. Driscoll [17]. This is our main tool for numerically calculating the function $g(z)$. We can now proceed to design the PDE backstepping boundary observer in the new coordinate system.

B. OBSERVER SYNTHESIS

The observer synthesis follows the same method used in section III. The only difference is that the transformed system is now defined in the geometry depicted in Fig. 3c, which corresponds to a cylindrical domain visualized in Fig. 4. The transformed domain features symmetry with respect to both ϕ and z axes and therefore results in the following (simplified) equation for the transformed system (1) in the new domain:

$$u_t = u_{\rho\rho} + \frac{1}{\rho} u_\rho, \qquad \rho \in (a, 1) \tag{11a}$$

subject to the boundary conditions as follows:

$$u(1) = 0 \tag{11b}$$

$$u_\rho(a) = \delta U \tag{11c}$$

$$u(a) = Measurement. \tag{11d}$$

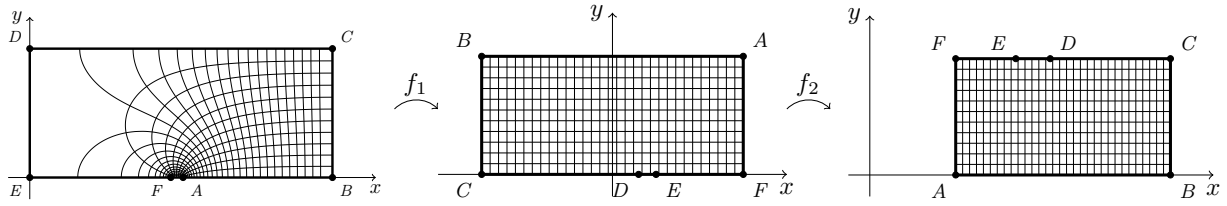

(a) Initial Geometry (b) Auxiliary Geometry (c) Final Geometry

Fig. 3: The illustration of the relationship between initial, auxiliary and final geometries. The mapping f_1 takes the auxiliary domain to the initial domain, while the mapping f_2 takes it to the final domain. Composition of the mapping f_2 with the mapping f_1 will take the initial domain to the final domain.

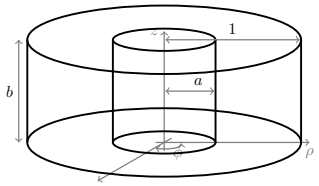

Fig. 4: The mapped domain Ω in the cylindrical coordinate system.

The PDE backstepping boundary observer design for the transformed system (11) is much easier than that for the original problem. We propose the following observer for the system (11):

$$\hat{u}_t = \hat{u}_{\rho\rho} + \frac{1}{\rho}\hat{u}_\rho + \ell(\rho)\left(u(a) - \hat{u}(a)\right) \tag{12a}$$

$$\hat{u}(1) = 0 \tag{12b}$$

$$\hat{u}_\rho(a) = \delta U + \ell_a\left(u(a) - \hat{u}(a)\right), \tag{12c}$$

where $\ell(\rho)$, and ℓ_a, are the coefficients to be designed. We define the observer error:

$$\tilde{u}(\rho) = u(\rho) - \hat{u}(\rho), \qquad \rho \in (a, 1) \tag{13}$$

which satisfies the following PDE:

$$\tilde{u}_t = \tilde{u}_{\rho\rho} + \frac{1}{\rho}\tilde{u}_\rho - \ell(\rho)\tilde{u}(a) \tag{14a}$$

$$\tilde{u}(1) = 0 \tag{14b}$$

$$\tilde{u}_\rho(a) = -\ell_a\tilde{u}(a). \tag{14c}$$

Equation (14) defines the observer error dynamics. The coefficients $\ell(\rho)$ and ℓ_a should be designed to stabilize (14). We look for an integral transformation:

$$\tilde{u}(\rho) = \tilde{w}(\rho) - \int_a^\rho P(\rho,\zeta)\tilde{w}(\zeta)\zeta d\zeta, \tag{15}$$

that transforms (14) into the following exponentially stable target system with desired dynamics:

$$\tilde{w}_t = \tilde{w}_{\rho\rho} + \frac{1}{\rho}\tilde{w}_\rho - \lambda^2\tilde{w} \tag{16a}$$

$$\tilde{w}(1, z) = 0 \tag{16b}$$

$$\tilde{w}_\rho(a, z) = 0. \tag{16c}$$

The function $P(\rho,\zeta)$ is the kernel of the integral equation proposed in (15). The parameter λ defines the observer convergence speed. Applying the standard PDE backstepping observer design, we obtain the following result:

Theorem 2: Let the PDE observer error dynamic in the cylindrical domain be defined by (14). Suppose that there exists an integral transformation (15) that can transform the error dynamics to (16). In addition, suppose that $P(\rho,\zeta)$ is the kernel of integral transformation where $a \le \zeta \le \rho \le 1$ describes the domain of the kernel function. Then observer parameters $\ell(\rho)$ and ℓ_a can be explicitly defined by the kernel function, $P(\rho,\zeta)$, and the kernel function itself can be calculated by solving the following PDE equation:

$$P_{\rho\rho}(\rho,\zeta) + \frac{1}{\rho}P_\rho(\rho,\zeta) + \lambda^2 P(\rho,\zeta) = P_{\zeta\zeta}(\rho,\zeta) + \frac{1}{\zeta}P_\zeta(\rho,\zeta), \tag{17a}$$

with the following boundary conditions:

$$P(\rho,\rho) = \frac{1}{2}\lambda^2\Big(1 - \frac{1}{\rho}\Big) \tag{17b}$$

$$P(1,\zeta) = 0. \tag{17c}$$

Proof: Due to space limitations, the proof is not provided here. The detailed proof is available upon request from the authors. ■

The exponential stability of the target system (16) and the invertability of the transformation (15) imply the exponential stability of (14) [12].

The domain of the PDE equation describing the integral kernel function is depicted in Fig. 5. Obviously, the observer parameter ℓ_a can be obtained from (14)– (17) as follows:

$$\ell_a = \frac{1}{2}\lambda^2\Big(a - 1\Big). \tag{18}$$

To complete the design we need to find the observer output injection parameter $\ell(\rho)$. For that, however, we need the kernel function, $P(\rho,\zeta)$,which requires solving the PDE equation (17). Since we do not have an analytical solution, we proceed with a numerical approach using the Finite Difference (FD) method. We calculated the approximate kernel function $\bar{P}$ using MATLAB. Next, we calculate $\ell(\rho)$ using $\bar{P}$ and employing backward difference calculation.

V. SIMULATION STUDY

To evaluate the performance of the designed PDE backstepping boundary observer, we presented simulation results for the transition starting from an initial stationary profile

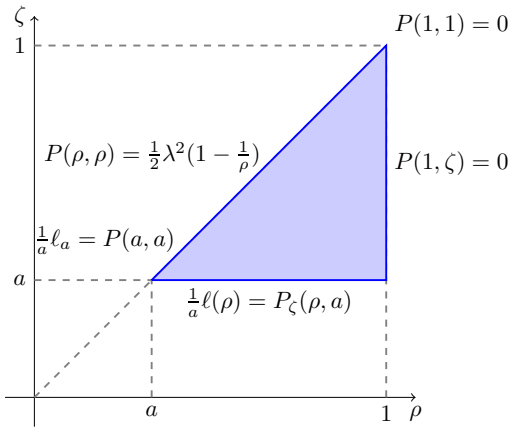

Fig. 5: The domain of the observer kernel $P(\rho,\zeta)$. Boundary conditions are showed at each boundary. The relationship between observer parameters $\ell(\rho)$ and ℓ_a with the bottom boundary and point at $\rho=\zeta=a$ are given as well.

TABLE I: The parameter values used in the PDE observer simulation

Parameter	Symbol	Value	Unit
Inner radius, Cylinder	a	0.25	mm
Outside radius, Cylinder	r_{out}	1	mm
Thermal diffusivity, Domain	κ	6.08×10^{-7}	m^2/s
Height, Cylinder	z	2	mm

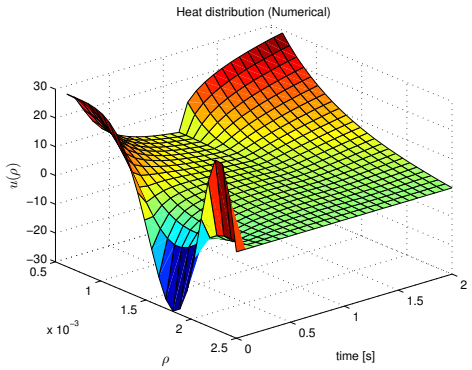

Fig. 6: Heat distribution in the domain

with a predefined input signal for the thermal system discussed in section II. To do this, in the first step the proposed observer is transformed from normalized space to its original space by rescaling spatial and temporal variables according to the physical parameters of the system (Table I). The input signal is constructed by a delayed unit step passing through a gain of $g=-114.7063$, equivalent to applying one watt of power. The delay is one second.

We used a sixth-order compact finite difference (CFD) scheme [18] in space and a fourth-order Runge-Kutta scheme in time to descretize the interconnected system for the simulation study. The chosen technique showed its merit in a simulation of PDE backstepping boundary observer designs [19]. The simulation is defined for a duration of

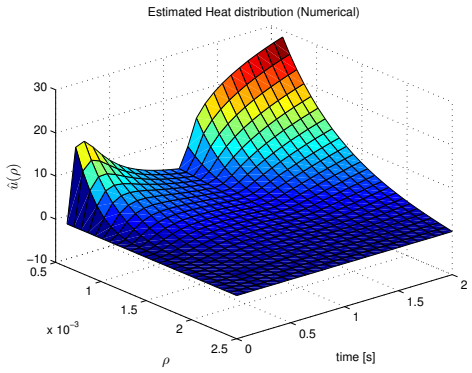

Fig. 7: Estimated heat distribution

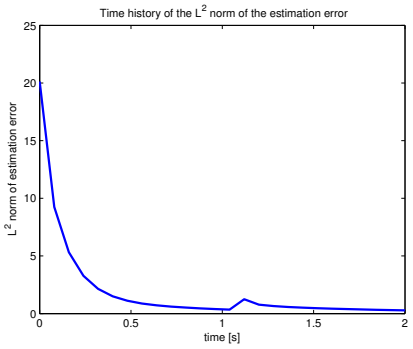

Fig. 8: Time history of the L^2 norm of the estimation error

2 seconds with 25 points time steps, which results in a 0.08-second temporal resolution. Similarly, the same number of discretization points, $N=25$, are chosen to discretize the spatial variable ρ. The initial condition is given by $u_0(\rho)=\cos(\frac{5}{2}\pi\rho^2)$.

As shown, the initial temperature decreased before the input pulse was applied to the system, which resulted in the subsequent temperature increase at the boundary.

For the observer system, we used a decay rate that was faster than the original system by choosing $\lambda=9$. Fig. 7 presents the dynamic heat distribution for the observer-system interconnected structure. To evaluate the performance of the designed observer, we calculated the L^2-norm of the estimation error and depicted it in Fig. 8 Specifically, the L^2-norm of the estimation error converged exponentially to zero and the small peak in the estimation error caused by the step input is well damped later.

VI. EXPERIMENTAL RESULTS

We chose a genetic analysis Lab-on-a-Chip (LOC) microfluidic chip [20] as the case study to evaluate the proposed technique. The analytical model for heat distribution inside the chosen microchip fits within the class of PDE systems considered in this work. Our goal is to estimate the temperature at specific points inside the microchip by measuring the boundary temperature and the amount of the applied power at the bottom boundary. Verifying the observer output, however, is nontrivial given that there is no direct

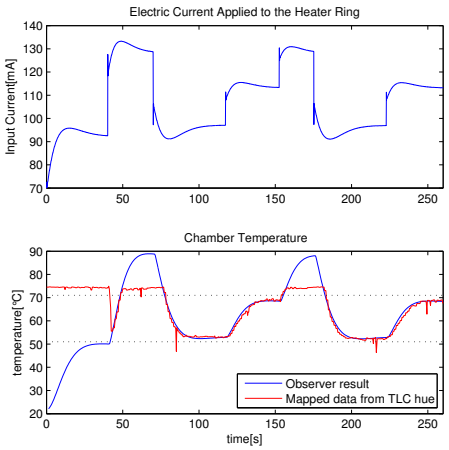

Fig. 9: Experimental results. The top graph shows the input current applied to the heater ring using a closed-loop PI controller. The bottom graph presents the observer results compared to the TLC's mapped hue readout from inside the chamber.

access to a conventional sensor inside the microchip. To solve this problem, we used experimental data collected during thermal characterization of our PCR-LOC microchip. The temperature characterization of a microfluidic chip is challenging, mostly because it is difficult to measure the temperature without causing significant perturbation. Thermochromic liquid crystals (TLCs) have proven their effectiveness in temperature measurement in microchips [21]. TLCs change color as their temperature is changing. We used R58C3W TLC (Hallcrest Glenview, IL, USA) with maximum sensitivity at 58°C, corresponding to the annealing stage of the PCR process in our experiment.

The TLC has a milky white color at room temperature. The TLCs turn red as the temperature rises to the lowest threshold of the color change range, green at the second temperature threshold, and blue at the third threshold. When the temperature rises above the color change range of the TLCs (about 70°C for the TLCs used here), the color returns to the original milky white color.

We used a SPZ-50 optical microscope and an L-150R60 fiber optical illuminator with ring light, in addition to a 3.1MP CCD camera to perform the experiment and to record the color change in the TLC during the PCR cycling. From the captured video, we transformed each frame to the HSV color space and mapped hue variations to temperature variations using the TLC's calibration curve. The result is depicted in Fig. 9. The TLC temperature reading within its bandwidth verifies the proposed observers accuracy.

VII. CONCLUSIONS

In this paper, we proposed an extension of the PDE backstepping approach to observer design for a special class of parabolic PDE systems. We showed that using the conformal mapping technique significantly reduces the calculation burden and makes it possible to design a PDE backstepping boundary observer in a complex cylindrical domain structure. Extensive simulations reveal the expected performance of the designed observer in terms of the errors L^2-norm. Higher performances can be achieved by changing the value of the λ in the design process. However, any increase in observer bandwidth should be carefully followed by properly selecting discretization parameters in the CFD method for further simulation or implementation. Finally, the proposed technique was applied to the observer design problem for a case study of a microfluidic system designed and constructed for PCR-based genetic analysis.

ACKNOWLEDGMENT

The authors would like to thank S. Poshtiban for performing the experiment and providing experimental data. This work is supported by the Natural Sciences and Engineering Research Council of Canada (NSERC).

REFERENCES

[1] M. Athans, "Toward a practical theory for distributed parameter systems," *Auto. Control, IEEE Trans. on*, 1970.
[2] S. Kitamura, H. Sakairi, and M. Nishimura, "Observers for distributed parameter diffusion systems," *Elec. Eng. Jap.*, vol. 92, 1972.
[3] R. Gressang and G. Lamont, "Observers for systems characterized by semigroups," *Auto. Control, IEEE Trans. on*, 1975.
[4] A. El Jai and M. Amouroux, "Sensors and observers in distributed parameter systems," *Int. Journal of Control*, 1988.
[5] Y. Liu, A. and L. Lapidus, "Observer theory for distributed-parameter systems," *Int. Journal of Systems Science*, 1976.
[6] I. Yaz, V. Bakke, and E. Yaz, "Receding window observer and dynamic feedback control of discrete infinite dimensional systems," in *Decision and Control, Proc. of the 30th IEEE Conf. on*, 1991.
[7] R. Miranda, I. Chairez, and J. Moreno, "Observer design for a class of parabolic pde via sliding modes and backstepping," in *Variable Structure Systems (VSS), 11th Int. Workshop on*, 2010.
[8] M. Cheng, V. Radisavljevic, and W. Su, "Output-feedback boundary control of an uncertain heat equation with noncollocated observation: A sliding-mode approach," in *Industrial Electronics and Applications (ICIEA), 5th IEEE Conf. on*, 2010.
[9] Z. Hidayat, R. Babuska, B. De Schutter, and A. Nunez, "Observers for linear distributed-parameter systems: A survey," in *Robotic and Sensors Environments (ROSE), IEEE Int. Symp. on*, 2011.
[10] A. Smyshlyaev and M. Krstić, "Backstepping observers for a class of parabolic PDEs," *Systems and Control Letters*, 2005.
[11] M. Krstić and A. Smyshlyaev, *Boundary control of PDEs: A course on backstepping designs*. Society for Ind. Mathematics, 2008.
[12] A. Smyshlyaev and M. Krstić, *Adaptive control of parabolic PDEs*. Princeton University Press, 2010.
[13] R. Vàzquez and M. Krstić, "Boundary observer for output-feedback stabilization of thermal-fluid convection loop," *Control Systems Technology, IEEE Trans. on*, 2010.
[14] J. Brown and R. Churchill, *Complex variables and applications*, 7th ed., ser. Churchill-Brown series. McGraw-Hill, 2004.
[15] L. Ahlfors, *Complex analysis: an introduction to the theory of analytic functions of one complex variable*. McGraw-Hill, 1979.
[16] P. K. Kythe, *Computational conformal mapping*. Birkhauser, 1998.
[17] T. Driscoll and L. Trefethen, *Schwarz-Christoffel Mapping*. Cambridge University Press, Cambridge, UK, 2002, vol. 8.
[18] S. Lele, "Compact finite difference schemes with spectral-like resolution," *Journal of Computational Physics*, 1992.
[19] D. Tsubakino and S. Hara, "Backstepping observer using weighted spatial average for 1-dimensional parabolic distributed parameter systems," in *18th IFAC World Congress*, 2011.
[20] G. Kaigala, M. Behnam, A. Bidulock, C. Bargen, R. Johnstone, D. Elliott, and C. Backhouse, "A scalable and modular lab-on-a-chip genetic analysis instrument," *The Analyst*, 2010.
[21] A. Chaudhari, T. Woudenberg, M. Albin, and K. Goodson, "Transient liquid crystal thermometry of microfabricated PCR vessel arrays," *Microelectromechanical Systems, Journal of*, 1998.